

# A Case for Hosted Space Domain Awareness (SDA) Sensors in MEO

**Daniel J. Petrovich, Matthew Sandnas, Jeff Pritchard**

*SEAKR Engineering & Raytheon Advanced Products & Solutions (APS)*

**Elvis Silva, Ken Johnson, Sonny Tahiliani**

*Blue Canyon Technologies (BCT), Raytheon Vision Systems, RTX Ventures, Raytheon APS*

## 1 ABSTRACT

A growing Medium Earth Orbit (MEO) hosted payload SDA market is overlooked and assumed suboptimal due to a historical bias towards dedicated SDA assets on the ground and in other orbits. The rise of MEO for commercial and defense capabilities lends itself to hosted SDA payloads in a more resilient environment with minimal debris, further from ground-based threats, and with unobscured visibility to LEO and GEO belts. Commercial SATCOM, GPS, Optical Crosslinks, and OPIR in MEO demands a commensurate increase in resilient, hosted space situational awareness. We provide a recommended hosted EO SDA sensor architecture to deliver detect and track of non-star objects above and below a given MEO constellation. Specifically, we propose the re-purposing of On-Board Processing (OBP) used by commercial MEO communications systems to serve defense SDA instrument(s). Such OBP electronics feature low recurring cost due to rate production, potentially eliminates redundant payload electronics, and reduces overall SWaP and integration costs. Data storage, processing, and dissemination of detected object messages is explored in support of future MEO SDA architectures. We demonstrate that a bootstrapped commercial OBP approach greatly reduces the downlink data bandwidth in cost and latency competitive compared to downlinking raw sensor data. Furthermore, we show that crosslinked MEO assets strengthen the existing SDA architecture by enabling low latency cross-cueing to deliver increased track quality to the broader SDA architecture.

## 2 INTRODUCTION

In this paper we explore a hosted, MEO-based SDA sensor that step-stare scans the GEO, MEO, and LEO belts for near persistent custody of manmade and natural objects. We explore the revisit rate, closely spaced object (CSO) capability, optimal constellation design options, and the visual magnitude and circular error of probability (CEP) limits of such a sensor. It is assumed that one sensor can perform both the GEO and LEO missions and that the sensor's primary focus is GEO and the secondary (suboptimal) focus is LEO. Additional MEO-to-MEO capability is not explored in this paper yet believed to be increasingly valuable as radiation hard components become increasingly used in the vast MEO orbit regime.

The step-stare sensor, based upon an existing design, is hosted on a MEO platform such as SSC's MEO Track Custody (MTC), on GPS space vehicles, or on a commercial MEO SATCOM spacecraft bus. It is assumed that multiple step-stare sensors, when properly manifested with favorable spacing would lead to 3D stereo track capability after fusion of angle-angle object sighting message (OSM) data in to unscented Kalman filtered tracks at a space or ground-based mission operations center (MOC). Crosslinked MEO space vehicles (SVs) are increasingly in consideration for commercial backhaul of data. Crosslink information sharing creates an incentive to form 3D track hypothesis in-space using on-board processing (OBP) to deliver more timely data products to MOCs or to tactical ground users on tactical timelines. Hosted OBP would need to survive a high radiation environment, so we provide an example baseline a SEAKR Sentinel 2.0 electronics unit and Raytheon Vision Systems (RVS) sensor focal plane capable of surviving the high dose environment. TRL-9 edge processed 3D tracks are leveraged from the STSS two-ball demonstration program, which crosslinked OSM data and performed on-orbit track fusion. We extend this technology to the MEO domain in service of the SSA and SDA mission.

Finally, we explore the data flow and operational concept of operations required to process and disseminate object sighting messages (OSMs) and tracks streaming from the hosted sensor to the OBP and back to the MOC for human-in-the-loop (HIL) flight operations. Valid tracks are adjudicated, and invalid tracks are dropped by USSF Guardians at the MOC or by commercial operators at a commercial MOC. Track fusion from other orbit regimes and/or from ground sites is performed to further increase track quality, custody, and persistence.

### 3 WHY MEO?

**The MEO hosted sensor marketplace:** The MEO regime today remains largely unexplored by commercial efforts and private funding. As a percentage of ever-expanding capital, indeed MEO's share percentage wise continues to shrink. Given high launch costs to MEO, this is unsurprising. However, as launch costs to LEO continue to shrink while tonnage to orbit increases (i.e., SpaceX's Starship), second-order effects may come into play. For example, as affordable space tug capability develops (i.e., start-up Impulse Space), new interest in MEO placed assets may emerge. According to FCC filing data, companies like Mangata Networks, O3B, and IntelSat envision operating satellite-enabled network and cloud service infrastructure stationed in MEO and HEO, augmented by terrestrial "edge" data centers. Conservatively, the MEO satellite market is projected to be worth USD \$9.52 billion by 2030, growing at a CAGR of 4.7% from 2023 to 2030.

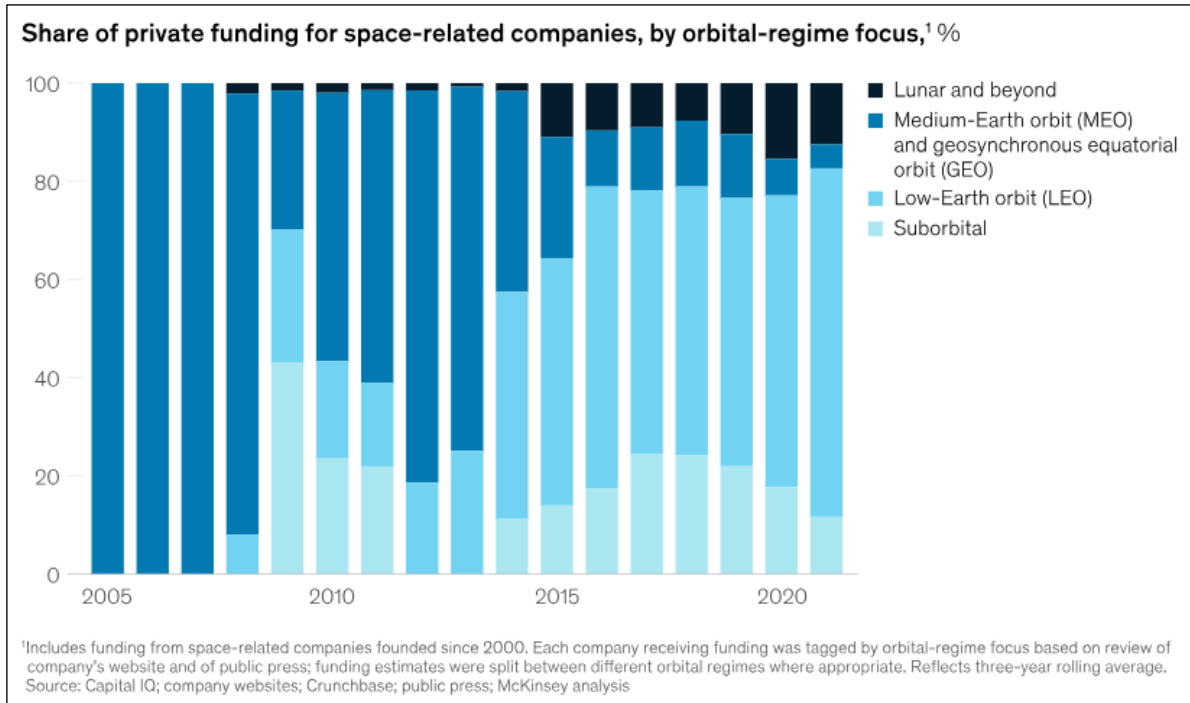


Fig. 1. Private funding timeline as a fraction of total dollars

Specific to in-space imaging for space domain awareness several companies operate or seek to operate in the segment including HEO Robotics (Australia), and U.S. based Maxar, OurSky, Scout Space, and True Anomaly (pursuit operations), however high resolution in-space imaging without rendezvous or revealed maneuvering remains largely allusive in MEO. Supporting infrastructure for data transfer and communications beyond LEO also remains a nascent segment, although in-space communications offerings are starting to be envisioned in the private sector. Demand from Five Eyes government customers exists today, with potential for commercial in-space traffic management rising in the future. Today, MEO remains a greenfield space domain awareness opportunity.

### 4 PROPOSED MEO CONOPS AND MISSION SYSTEM ARCHITECTURE

This paper presents a novel approach to space object tracking and correlation using a hosted payload that returns angle-angle tracks. A constellation of MEO satellites, providing unique look angles to many of the orbits of interest can provide multiple looks from different locations to generate the angle-angle tracks as shown in the OV-1 of a hosted SDA sensor on a low-MEO satellite communication satellite in Fig. 1. This is done autonomously (Scan mode) and semi-autonomously (Task mode) in conjunction with hosted payloads on other satellites in the constellation as shown in Fig. 2. The hosted payload's onboard processor (OBP) receives a database of objects from the ground. The OBP then propagates the objects in the database to the current time. The OBP compares the observations of detected objects to the propagated database of objects. If the observations match an object in the

database, the OBP correlates the identified object in the field of view. If the observations do not match an object in the database, the OBP sends an exceedance alert to the ground. The system further aims to improve the accuracy and certainty of space object correlation through several techniques discussed below.

**Satellite Constellation Configuration:** The study utilizes a sample constellation for analysis, specifically a medium Earth orbit (MEO) configuration with twenty-one (21) low-MEO space vehicles (SVs) and four (4) high-MEO GPS SVs per orbit plane. One orbit plane is considered to improve readability. In Figure 1 we performed a stereo viewing Monte Carlo analysis of MEO to GEO observations with the assumption that one low-MEO SATCOM orbit plane with four (4) hosted payloads is leveraged to observe the GEO belt.

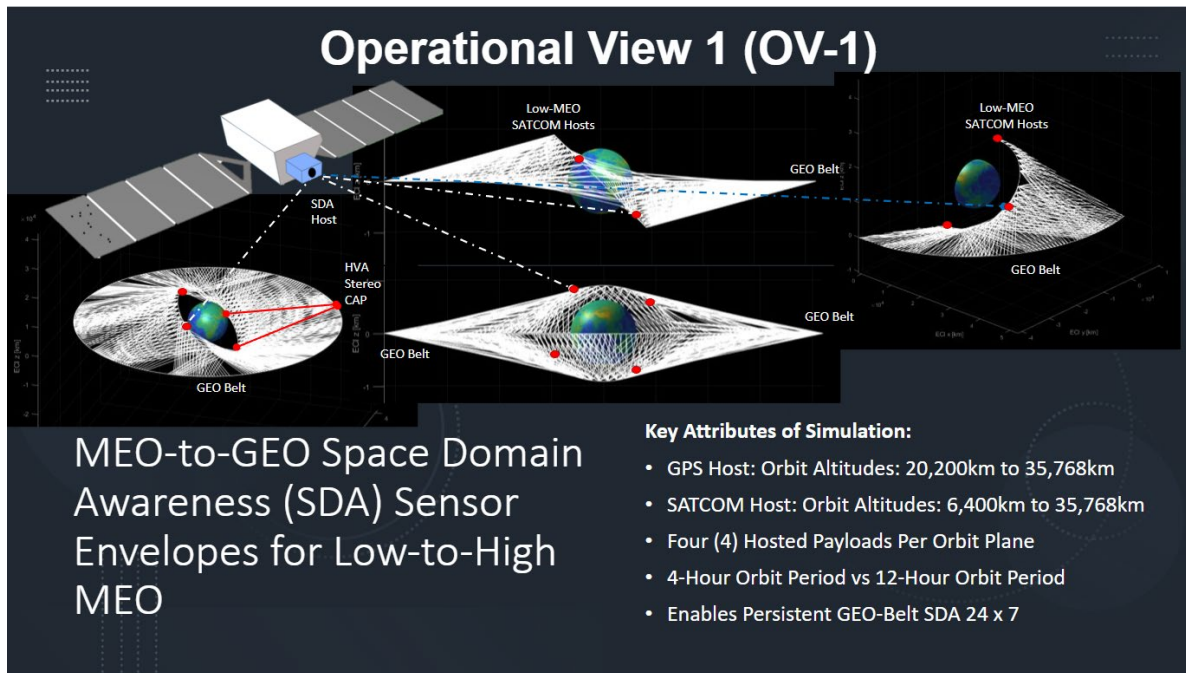


**Fig. 2.** Operational view-1 (OV-1) of MEO-to-GEO space domain awareness (SDA) sensor envelopes for low and high MEO hosted instrument mission scenarios. Low MEO is often dominated by SATCOM or OPIR hosts and high MEO is dominated by PNT constellations.

**Onboard Database updates:** The OBP proposed in our MEO concept provides the capability to accept regular updates of a known object database to use for correlation of space object observations. These databases are important to maintain and accurate catalog of known objects in GEO and as a reference to compare observations to. A regular cadence of updates to this database will be needed to minimize the probability of false detections to further optimize the value of the onboard processing function. The OBP database can be updated entirely at one time (i.e., during major maintenance upgrades) or individual records can be updated as objects are refreshed from ground observations and other sources.

Ground operators would schedule these regular updates on the basis that minimizes the amount of data that needs to be uploaded and the amount of ground resources needed to support these updates. Beyond parameters related to estimated state for each object in the catalog, other parameters such as state uncertainty and time since last update can be included to further enhance the utility of the GEO catalog.

**Space Object Tracking and Correlation Methodology:** A function of the OBP is to correlate detected object with objects from the on-board database. This process serves to reduce uncertainty and enhance the reliability of tracking and identifying space objects. This is done through two fundamental methods: 1) Estimation of an object's state with multiple samples and 2) by gathering angle-angle tracks with the help of neighboring hosted payloads, and processed to estimate an object's state with multiple observers and samples. The first method evaluates multiple images taken as the host itself propagates among its MEO orbit. This is a common method that can estimate state of an object using various estimation techniques as the Resident Space Object (RSO) and/or the host propagate along a given trajectory Wu [1]. The second method will further improve the correlation accuracy by requesting another hosted payload in the constellation, which we will refer to as host B here, to detect the object of interest. The look vector and range from the current host (Host A) to RSO are passed to the requested Host B, which uses that

information to determine a region for which to search for the RSO in question. If a range estimate is not available, the Host B can step stare from Host A along the Host A look vector until a candidate object matches the characteristics of the RSO in question. The system can then acquire angle-angle track information, thereby increasing the certainty of correlation with the known object database.

**Ground Operations and Object Correlation:** In conjunction with the space-based operations, ground operations play a crucial role in maintaining the accuracy of the database. Uncorrelated objects are reported to ground operations at a time of convenience, enabling further investigation of the uncorrelated RSO. Moreover, ground operations can request the return of correlated objects, which contributes to an increase in the fidelity of the database as proposed by Blake [4]. The enhanced frequency of observations leads to a more robust database, facilitating improved tracking and identification of space objects.

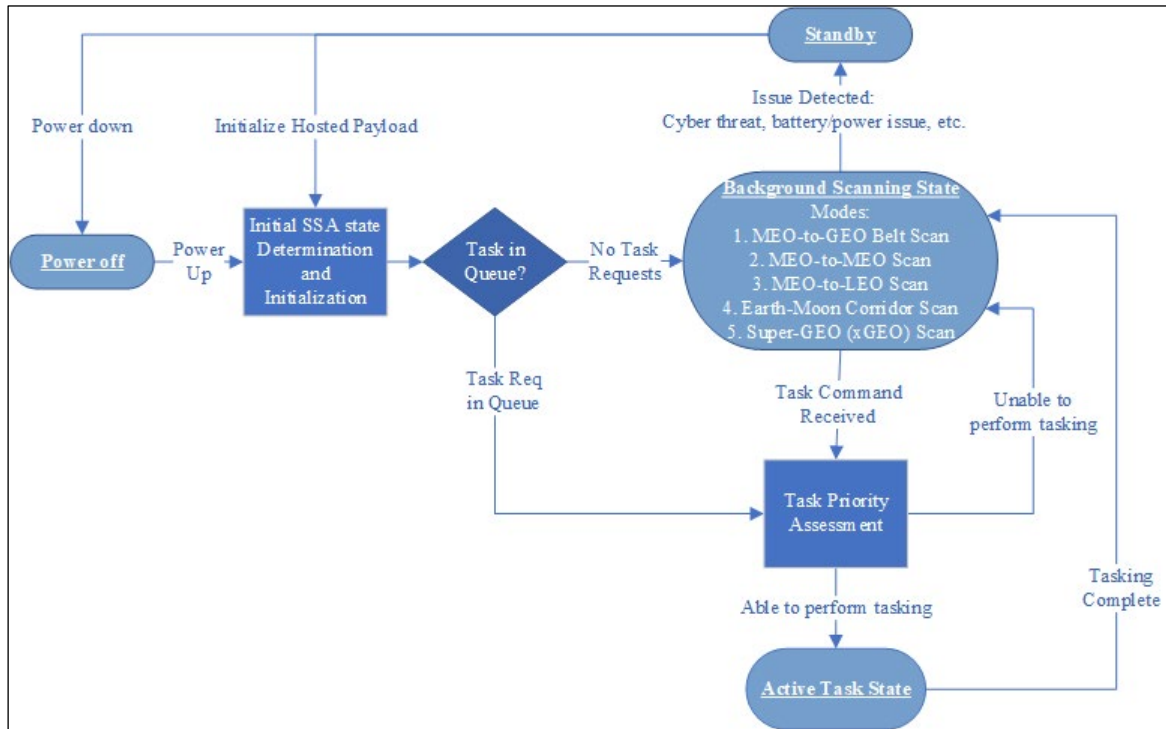


Fig. 3. Top-level logical flow of the states and modes

**Design Reference Mission:** This paper introduces two payload states and five modes for the first state; background scan. For the second payload state, one mode exists: task mode. These states and modes encompass a variety of capabilities targeting different orbits, such as Geostationary Earth Orbit (GEO), Medium Earth Orbit (MEO), Low Earth Orbit (LEO), Earth-Moon corridor, Super-GEO scan, and Task Mode. The paper focuses on evaluating the efficiency and benefits of these states and modes, particularly the GEO Belt Scan and Task Mode related to GEO belt tasking.

### Background Scan Payload State:

1. **MEO-to-GEO Belt Scan Mode:** The GEO Belt Scan mode is designed to automatically and incrementally scan the Geostationary belt to identify new unidentified objects and correlate known objects. By continuously monitoring this critical region of space, these modes aim to ensure comprehensive situational awareness and improve the ability to track potential hazards within the GEO belt.
2. **MEO-to-MEO Scan Mode:** MEO scan mode is instrumental in protecting the satellite constellation itself and other objects in the MEO regime. This mode involves monitoring crossing orbits and looking ahead and behind the satellite constellation to detect potential hazards.

3. **MEO-to-LEO Scan Mode:** The MEO-to-LEO scan is similar to the GEO belt scan, but it is more limited by lighting conditions and relative orbit rates. It can only observe objects well above the earth limb in favorable lighting conditions. The relative orbit rates between the objects and the observer affect how well our sensor can correlate these object tracks to the database.
4. **Earth-Moon Corridor Scan Mode:** The MEO orbit offers a unique advantage in earth-moon corridor SDA, because of wide-angle observer location diversity, which delivers low RMS error for circular area of probability stereo tracks. It also delivers the advantage of unique lighting conditions and observation times that Earth, LEO, and GEO cannot provide.
5. **Super-GEO (xGEO) Scan Mode:** Unlike the Earth-Moon corridor scan, the xGEO scan is unconstrained from the earth-moon corridor region. The xGEO scan is focused on the area beyond GEO and away from the equatorial plane, to monitor for objects with high equatorial elevation angles at and beyond GEO.

**Active Task Payload State:**

6. **Task Mode:** The task mode is a versatile mode that allows for time sensitive SDA collects within the sensor sensitivity range. One practical application of the task mode is to observe neighboring satellites to search for nearby debris or threats. Another application is active step-stare observation at high frame rate of suspect collision threats or debris via conjunction. The use of angle-angle track correlation enhances early warning capabilities and reduces the data dimensionality to reduce downlink communications cost. Stereo track can see changes in orbit motion that could indicate increased threat risk. Stereo track fusion is expected to be performed at the ground ops center unless crosslinks exist between MEO assets.

## 5 MEO SENSOR RECOMMENDATION(S)

We explore a high-MEO GPS-hosted and low-MEO SATCOM hosted SDA sensor at distinctly different orbital altitudes and characterize the sensor-frame rotation relative to the GEO belt. In the MEO industry we see satellite communication dominating low MEO and PNT dominating high MEO for physics-based reasons. These host markets create opportunity for lower cost hosted SDA sensing. Below, we characterize the stereo observation angles and rate of revisit for all know GEO satellites. The GPS constellation simulations consist of four (4) sensors per orbit plane; one on each GPS space vehicle. The low-MEO-hosted SDA sensors consists of 21 space vehicles of which four (4) equally spaced sensors are hosted. The GPS orbit is one every 12-hours whereas the low-MEO orbit period is four hours, roughly 6000km orbit altitude. This results in a higher revisit rate for GEO HVAs compared to GPS, but lower quality observations from the relatively longer range to GEO from the low-MEO orbit. The sensor selected is given in Figure G and is equipped with a 2.65 x 1.47-degree field of view imager with high quality SB501 focal plane array (FPA). The GEO belt is repeatedly scanned with a step-stare approach that scans the camera frame up and down the GEO belt at one step-per-second to the maximum range limit of 36,000km. Step-stare scans up and down the GEO belt are conducted during the relatively slow MEO orbit (as compared to LEO), which leads to an aggregate revisit for all GEO objects of interest and a very high rate of stereo observation revisit.

Parameter	Value	Units	Notes
Single Camera FoV	2.65° × 1.47°	deg	
Camera Pixels	8192 × 2048	pixels	SB501
Instantaneous FoV	1.3	arcsec	per pixel
Operating Power	156	Watts	
Required Mass	100	kg	20% Reduction
1σ Uncertainty	0.65	arcsec	Inertial Est
Mounting	2-axis Gimbal		

**Figure 4.** Example SDA Sensor with Raytheon Vision Systems (RVS) Focal Plane Array (FPA) Specifications and SEAKR Engineering On-Board Processing (OBP) Electronics



The relative rotation of the sensor to the GEO belt is characterized vs. time and must be considered for future design implementation, since seamless coverage of the GEO belt is driven by the rotated tile overlap of step-stares. Guaranteed time correlated stereo observations of HVAs and closely spaced objects (CSOs) must also take into consideration the rotated nature of the sensor reference frame to the GEO belt such that priority observations are both in-scene at the time of the stereo collect. Apps that reside in the Mission Ops Center (MOC) in support of the mission planning cycle are to consider sensor unique constraints.

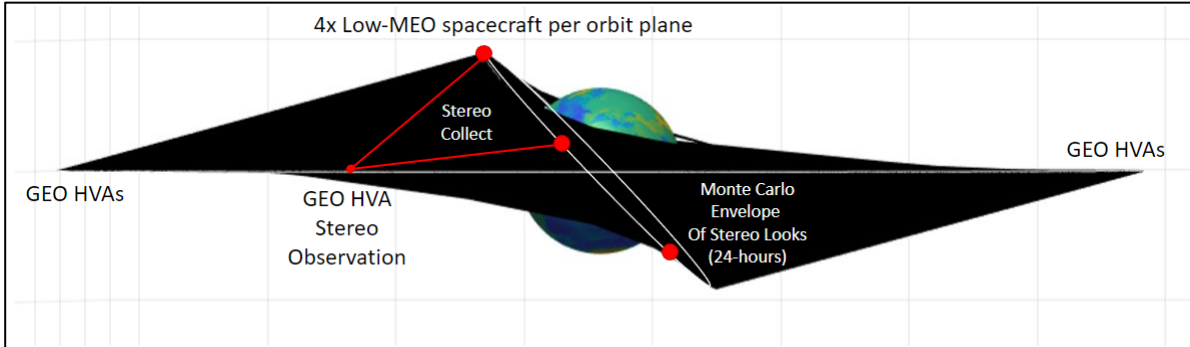


**Figure 5.** 24 x 7 GEO-belt SDA sensor line of sight vectors in the ensemble create a dense volume of 3D stereo view of the GEO belt [observed edge-on to the equatorial plane]. Orbital inclination of the low-MEO observer sensors creates high and low observation geometry to further improve stereo observation quality.

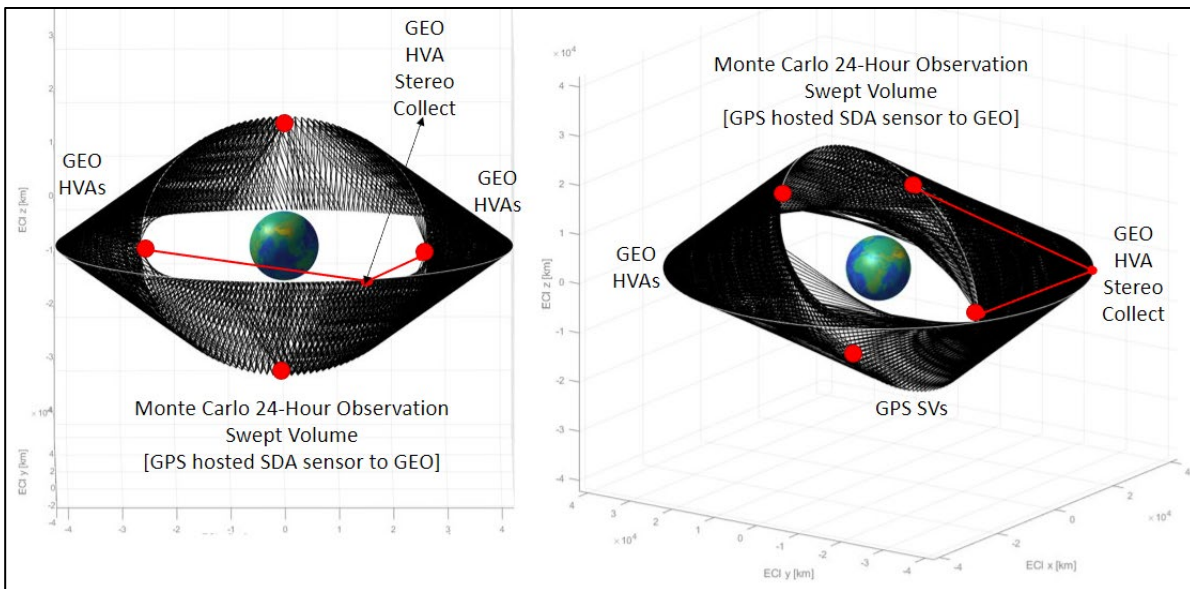


**Fig. (6a)(6b).** Stereo observations of the GEO-belt from GPS in high-MEO swept out over a 24-hour period demonstrates the diversity of viewing opportunities with only one orbit plane containing four (4) SVs.

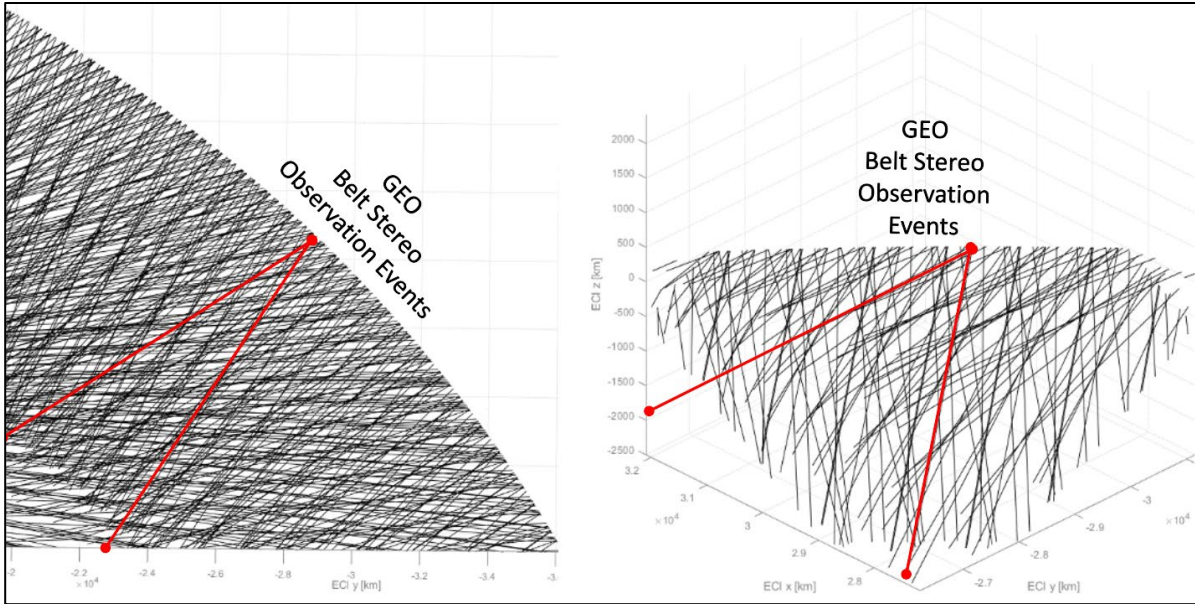


**Fig. (7a)(7b).** Stereo observations of the GEO-belt from GPS in high-MEO leads to 24 x 7 persistent coverage of the belt with better viewing geometry compared to Earth-ground, LEO, GEO, and GEO+ observation locations.

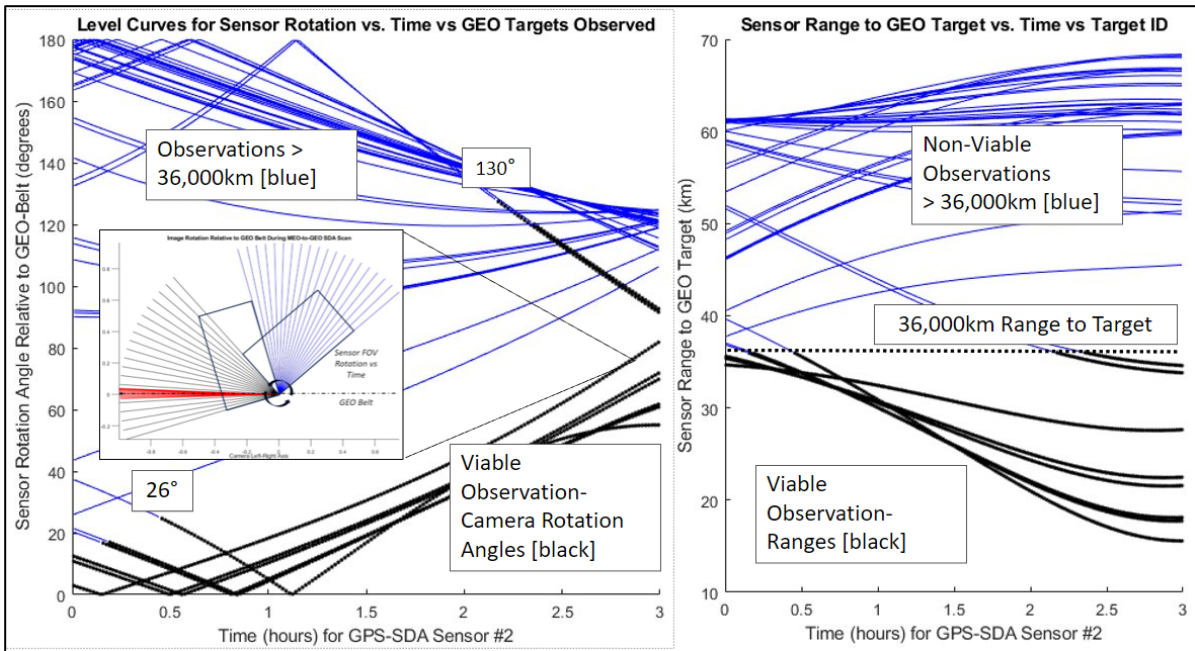


**Figure 8.** For a GPS hosted SDA sensor that completes 1/4<sup>th</sup> of a 12-hour orbit, the sensor region of interest (ROI) rotates [left plot] relative to the GEO plane (Y-Axis) as the range to target [right plot] increases and decreases as a complex function of GPS satellite inclination and orbital altitude. Range is limited to 36,000km [black].

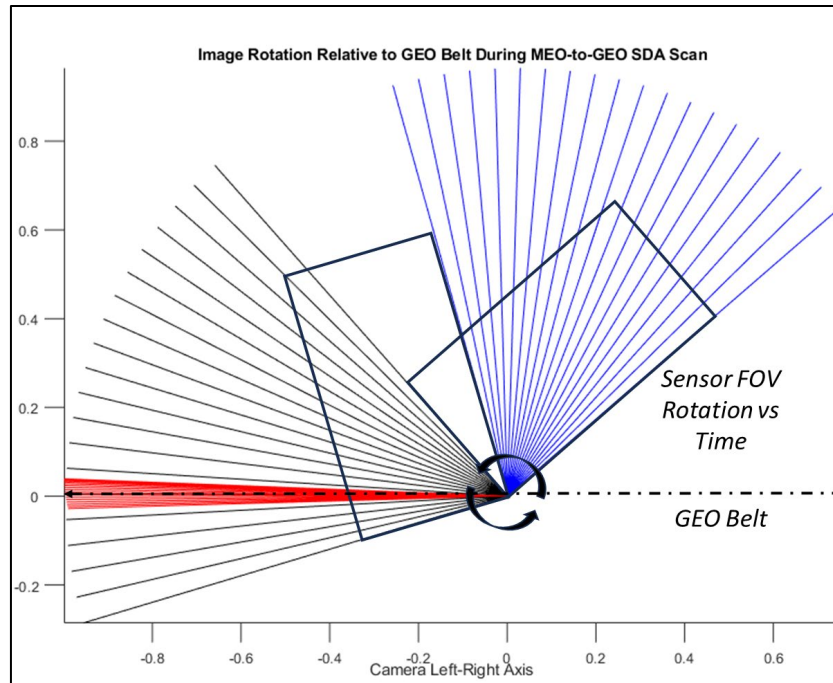


**Figure 9.** Sensor camera orientation [blue X-Axis, black Y-Axis] rotates relative to the [red] GEO belt vector over time. Low-MEO rotation rate is higher than High-MEO rotation rate by a factor of approximately 3x. Sensor relative rotation creates an opportunity for improved matched filter detection of non-star RSOs.

## 6 CONSTELLATION DESIGN: OBSERVATION GEOMETRY MATTERS

**Figure 11** defines coordinate systems that relate constellation design choices,  $altOb$  (observer altitude), observer central angle  $\Phi$  ( $360/nSat$ ), and relative target location  $T(\theta, \phi)$ , to the error ellipse defined by the covariance matrix  $\Sigma$ . Computing error over target position for sets of typical altitude and  $nSat$  it's easy to show that the selection of  $altOb$  and  $nSat$  have a huge influence on how well a constellation configuration can estimate the position of any given target. This is seen in the large cyclical swings in the time domain plot of RMS Error for six constellation configurations orbiting at a 33-degree inclination observing an equatorial GEO target. A thoughtful look at the epipolar angle  $\varepsilon$  in the vector diagram of **Figure 10**, and its appearance in the covariance matrix  $\Sigma$ , shows that RMS Error is minimum when  $\varepsilon = 90$ -degrees. Thus, observation geometries that maximize the amount of time  $\varepsilon = 90$ -degrees as observers and targets orbit, minimize RMS Error.

Using the standard definition of Expected Value (EV), we compute expected RMS Error and densities (see whiskers shown in the right of **Figure 11**) over all GEO target locations for seven constellations ranging from LEO thru GEO. These were computed assuming a composite jitter  $\Sigma = 1$  uRad. Per the derivation of  $\Sigma$ , results in **Figure 11** scale with  $\Sigma$ . The results show that due to geometry alone, HMEO thru GEO constellations perform the GEO SSA mission with 4x to 10x lower RMS Error than constellations at LMEO and below. Conversely, HMEO thru GEO constellations perform the LEO SSA mission with 4x to 10x higher RMS Error than constellations at LMEO and below.

To determine the optimal altitude for the GEO and LEO SSA missions we selected  $2 < nSat < 24$  and determined the altitude that minimized EV using a standard gradient decent algorithm.

Summary results are as follows: for  $2 < nSat < 8$  altitudes that minimize the GEO SSA mission RMS Error range from 25,000 to 29,000 Km. At those optimal altitudes there is minimal sensitivity to  $nSat$  with a shallow bowl around  $nSat = 5, 6, 7$ .  $nSat > 8$  results in central observer central angle  $\Phi$  reducing the length of baseline  $a$  and epipolar angle  $\varepsilon$ , resulting in increasingly higher Expected RMS Error. As shown in the plot on the right of **Figure 11**, the constellation that produces the minimum Expected RMS Error for the GEO SSA mission is:  $nSat = 6$ ,  $aOptGEO = 29,270$  Km. The constellation that produces the minimum Expected RMS Error for the LEO SSA mission is:  $nSat = 6$ ,  $aOptLEO = 312$  Km. Looking at a typical set of GEO SSA time domain error plots for  $aHMEO$  and  $aOptGEO$  on the right of **Figure 10**, it's clear that for several hours the optimal constellation provides substantially lower error



due to the superior observation geometry of that constellation. As the epi-polar angle  $\varepsilon$  passes 90-degrees, custody is handed off to next observer pair in the plane,  $O2 - O3$ . The LEO SSA mission results behave similarly. It interesting to note that, like the GEO SSA mission, the optimal LEO SSA altitude is below the targets being observed.

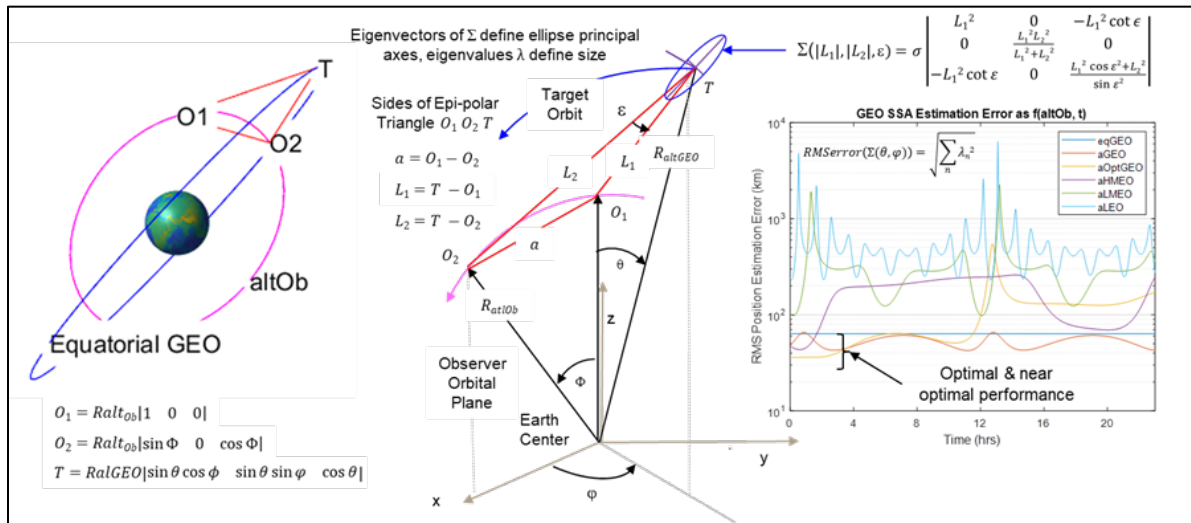


**Fig. 10.** Polar coordinate frame geometry reveals optimal constellation configurations in MEO for stereo SDA. Closed form solution for optimal viewer location(s) enables high speed lookup table (LUT) algorithms in cloud or OBP-based mission planning tools.

**Figure 10**– The key to quantifying measurement performance is understanding the red epi-polar triangle defined by Observers 1 and 2 and the target T. As shown by the covariance matrix  $\Sigma$ , when the epi-polar angle  $\varepsilon = 90$  degrees, the off-diagonal  $\cot(\varepsilon)$  terms are zero. Time domain plots of RMS Error over a 24 GEO period show that error varies by orders of magnitude depending on one’s choice of observation geometry.

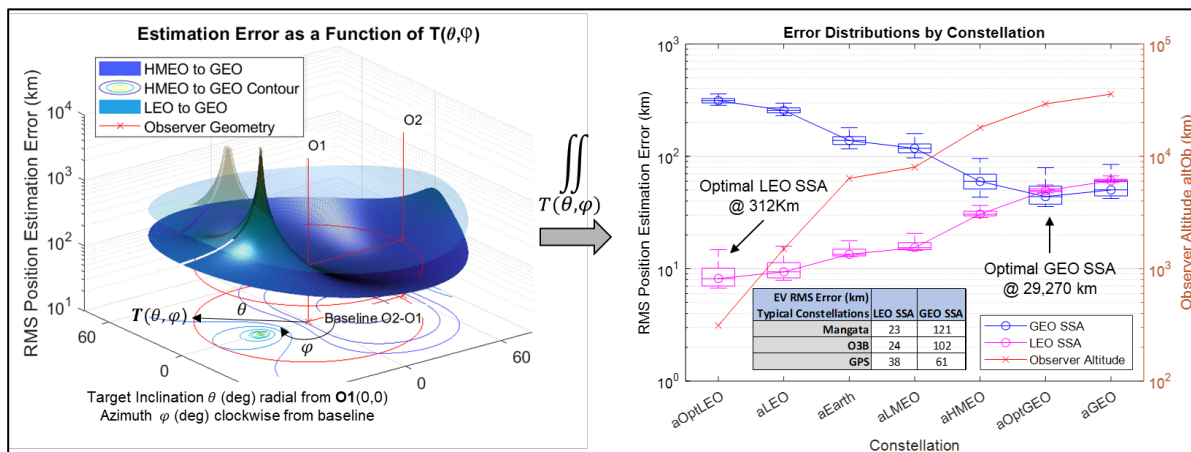


**Figure 11** – Polar (Target inclination  $\theta$  is radial from  $O1$ , azimuth  $\varphi$  rotates clockwise around from  $O1$  from baseline  $a$ ) surface and contour plots of RMS Error are smooth over  $T(\theta, \varphi)$  with a minimum along the baseline  $a$  between the observers. The large poles are geometries where  $T$  is colinear with  $O1$  and  $O2$ . On the right, integrating over the probability that  $T$  is located at  $(\theta, \varphi)$  produces RMS Error density and expected value for the GEO SSA and LEO SSA missions at seven altitudes. Minimizing the objective function shows that for the GEO SSA mission,  $\Phi = 60$ -degrees ( $nSat = 6/\text{plane}$ ) and  $altOb = 29,000$  Km ( $aOptGEO$ ) minimizes RMS Error over all target positions. For the LEO SSA mission, assuming a target orbit of 1500 Km, the minimum is  $\Phi = 60$ -degrees ( $nSat = 6/\text{plane}$ ) and  $altOb = 312$  Km ( $aOptLEO$ ).

## 7 ENABLING THE MEO SDA ARCHITECTURE WITH ONBOARD PROCESSING

However, significant challenges pertaining to performing SSA and SDA in MEO constellations still exist and need to be overcome if such constellations are to be seriously considered. These considerations include:

- Necessity for substantial data transfer to ground stations for processing identified orbital trajectories.
- Cost implications of establishing and maintaining uplink and downlink connections.
- Cost of operators in control centers
- Management of operator workloads.
- Coordination of observational efforts among diverse platforms.

These hindrances have historically rendered the economic viability of such systems unfavorable. However, recent advancements in onboard processing and autonomous operations present opportunities to surmount these limitations. This section delves into the viability of a system that harnesses onboard processing within hosted payloads to facilitate the realization of an effective Space Situational Awareness (SSA) architecture.

### 7.1 MOTIVATION FOR ONBOARD PROCESSING

Onboard Processing provides the opportunity to greatly reduce the data communication bandwidth. The example SB501 8K x 2K staring sensor generates 14-bit pixels. Each step-stare scan generates 235 Mbits of data. Even at a 1 Hz step rate, the sensor generates over 20 Terabits of raw information in a 24-hour period. Within the proposed constellation of 28 platforms, the amount of data approaches 570 Terabits, or 70 Terabytes per day. The cost associated with downlinking this amount of data for ground-based processing is unaffordable. Starlink has a target price of \$500.00 per month for a 220 Mbit/sec link, or about \$23.00 per Mbps per month (<https://www.starlink.com/business>). Data caps may apply. With sufficient onboard processing and storage resources, the required data rate can be greatly reduced by supplying information only about non-RSOs that are not in the catalog maintained in the OBP. The total yearly cost of downlinking raw image data would be approximately \$230M/year compared to \$7M or less for object sighting messages (OSMs) only and an order of magnitude less if angle-angle tracks only.

### 7.2 ON-BOARD PROCESSING HARDWARE DESCRIPTION

A notional On-Board Processor is an architecture that optimizes size, weight, power and cost (SWaPC). This processor is depicted in **Figure 12**. The OBP is derived from products developed for various Space Development Agency proliferated transport and tracking constellations. The architecture supports a flexible mix of instruction set processing on a single board computer (SBC), storage, and FPGA based processing slices. A small form factor allows easy deployment as a hosted payload on a wide variety of spacecraft bus configurations.

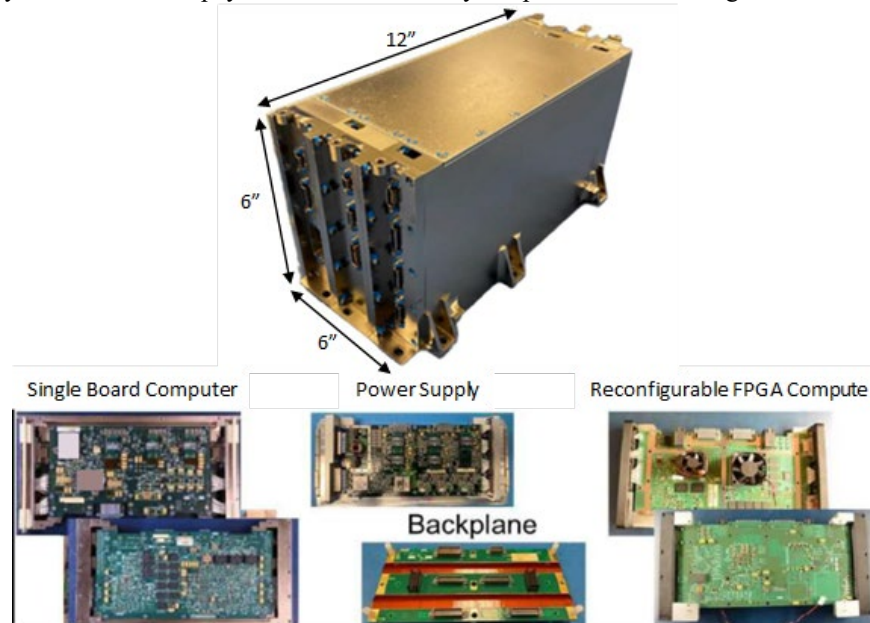


**Fig. 12.** Example on board processor (OBP) and representative slice

The single board computer uses multi-core commercial microprocessors that have demonstrated acceptable radiation performance for use in the MEO environment and score 12,000 – 20,000 on the CoremarkPro benchmark. These processors can be coupled with 16-32 Gbytes of DDR4 SDRAM and 100's of Gigabytes of local nonvolatile storage. They also feature integrated networking functions, allowing easy integration to the satellite communication systems such as inter-satellite links on modern, IP based platforms.

Reconfigurable FPGA processing slices host SRAM based reprogrammable FPGAs and SONOS Flash based FPGAs that retain their configuration over a power cycle. External interfaces of both FPGA types include multiple lanes of High Speed SERDES, well suited for a direct focal plane interface, PCI Express for connectivity to other slices in the OBP and 1 Gigabit and 10 Gigabit Ethernet IP based interfaces for connectivity to the instruction set processor and inter-satellite links. SRAM based FPGA resources include instruction set and vector processing units. An example device is the AMD-Xilinx VC1902 device which is being offered in a space-grade part suitable for the MEO environment. This device features 2 ARM A72 processors, 2 ARM R5F real-time processor cores, FPGA fabric with 900,000 LUTs, 256 Kbytes of ECC protected memory, and 400 Very Long Instruction Word, Single-Instruction Multiple-Data vector processors. These resources are connected via a high-bandwidth Network-On-Chip fabric. FPGA based processing can be an order of magnitude more power efficient than commercial GPUs. The device is well suited for pixel normalization functions on the raw image, such as non-uniformity correction, and bad pixel replacement. Then it can perform centroid clustering and then pass exceedance clusters to the single board computer slice via low power, high speed serial interfaces.

A non-volatile memory (NVM) slice with 2-3 Terabytes of storage is also part of the OBP architecture. The slice approach, using a radiation tolerant FPGA as a controller, is far more reliable than SSD based approaches, especially in the harsh radiation environment of a MEO constellation. Hewlett Packard Enterprises experienced multiple SSD failures when they deployed an unmodified commercial off-the-shelf (COTS) high-performance computer and sent it to the International Space Station (ISS) [5]. “The space environment also took a particular toll on SBC-1’s solid-state disks—out of 20 solid-state disks, 9 failed during the mission. The system had redundant copies of all data, so no data was lost, but the team plans to try different methods to better protect the solid-state disks during the SBC-2 mission.” This storage asset can be used to hold reference data, such as relevant portions of the Two-Line Element (TLE) Space-Track database and a 600GB Gaia star catalog and still have sufficient capacity to record and forward raw sensor data for a significant portion of the host platform’s MEO orbit. Multiple NVM slices can be added to the architecture for greater capacity.

### **7.3 ON-BOARD PROCESSING FIRMWARE AND SOFTWARE OVERVIEW**

The overall processing flow is shown in **Figure 13**. This results in an astrometric mission data processing platform with significant star-processing capability for Above-The-Horizon (ATH) containing both stars and targets. The onboard firmware (FPGA) processing creates calibrated images by normalizing (desaturation, spike removal non-uniformity correction and integrating (co-add) the raw sensor data. These are typical onboard processing steps for sensor interfaces and do not contribute significantly to data reduction, but the calibrated images can be stored in the NVM slice for cases when it is desired to downlink the full image data. In the second step of processing, a relevant portion of the star catalog is retrieved from nonvolatile bulk memory. The FPGA performs frame alignment (including rotation compensation), star deletion, background subtraction and enhanced star scene processing such as matched filtering and adaptive thresholding. Finally, exceedances are determined, and are passed to the multi-core instruction set processor for track generation, and to provide feedback to the bus computer for continued alignment to the active track for subsequent step-stare samples. Object sighting messages (OSM) can be formatted and stored in the NVM, correlated and downlinked with the normalized full scene image for validation or tuning of the exceedance processing with a ground based digital twin.

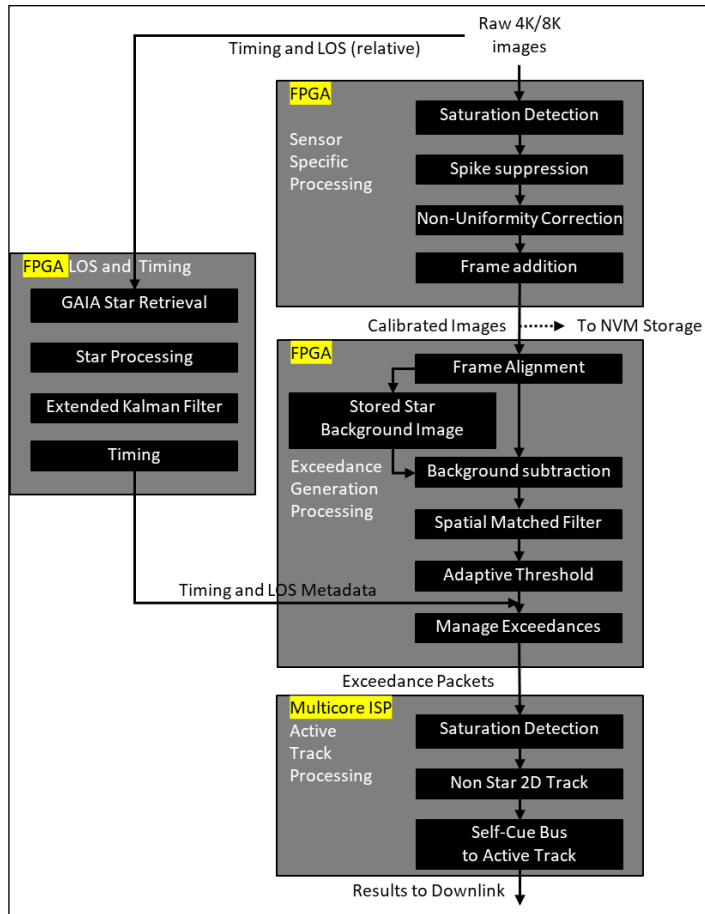


**Fig 13.** Firmware-software processing flow

The on-board processing results in a significant data reduction as depicted in **Figure 2**, resulting in a much lower cost of operation when compared to downlinking multiple frames of calibrated images.

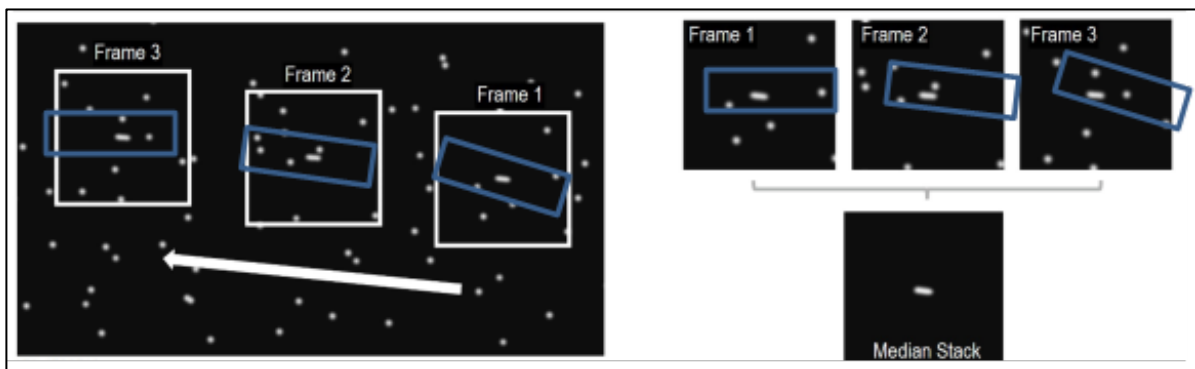


**Fig 14.** Data reduction thru on-board processing.

## 7.4 OPERATIONAL PROCESS FOR PROPOSED CONOPS

The intricate inter-workings of mission CONOPS are often tailor-fitted to suit the unique demands of the various operational modes of a mission. This malleability allows for efficient functioning across a spectrum of scenarios, ensuring that each Design Reference Mission's distinct requirements are meticulously met. In the context of the concepts described within this paper, we delve into two system operational modes supporting the six (5 + 1) sensor modes defined previously, *background scanning mode* (**Figure 15**) and *active tasking mode* (**Figure 16**).



**Scanning Mode:** The scanning mode, functioning autonomously, is primarily established by ground operators, and continues indefinitely based on various host spacecraft's state parameters, relative to the orbital regime being observed. This mode continues its operation unless prompted by ground operator intervention, receives a request from a fellow hosted payload within the constellation, or through the exit due to maintenance or anomalous condition. Notably, it features an autonomous capability to promptly notify ground operators of newly detected objects, offering an efficient mechanism for tip/cue utility to other hosts or other assets beyond the host constellation. The following process flow diagram outlines the scenario for automatic tip/que coordination and the subsequent object position determination and correlation:

- **Step 1: Determine Sub Mode and Region to Scan:** The space vehicle (SV1) determines which area to scan. This is done through configuration settings (I.e., which sub mode per section 4) and the last region scanned as stored recorded in memory.
- **Step 2: Object Detection by SV1:** SV1 detects a space object within its area of responsibility (AOR), removing known stars as indicated by the star map for this region as seen from SV1's current location in orbit.
- **Step 3: Attempting Correlation with Known Database:** SV1 attempts to correlate the detected object with its known database of space objects. However, if SV1 cannot establish a correlation, further measures are taken. To correlate the positions of known (i.e., cataloged) RSOs, we propagate their positions using two-line elements (TLEs) together with the US Space Force (USSF) Simplified General Perturbations #4 (SGP4) propagator orbital model to obtain current time position and streak estimates of each object within the AOR.
- **Step 4: Neighboring Satellite (SV2) Engagement:** SV1 determines SV1 initiates communication with neighboring satellites, such as Space Vehicle 2 (SV2), to request assistance in detecting and correlating the object. Automatic tip/que coordination with other MEO SSA assets enables triangulation of objects for better object position determination / track correlation without increased demand on space-to-ground communications and increased operator workload.
- **Step 5: Object Detection by SV2:** Upon receiving the request from SV1, SV2 scans the specific target AOR and attempts to detect the same object. This is achieved by step-staring along a track hypothesis region along the line of sight of SV1 using SV2's instrument. A priori knowledge from candidate database objects helps to reduce the distances along such a vector and thereby reduces that average time to find the referenced target.
- **Step 6: Information Sharing between SV1 and SV2:** SV1 and SV2 share their detection information with each other. This exchange of data enables a more comprehensive understanding of the object's characteristics and trajectory.
- **Step 7: Three-Point Object Correlation:** Both SV1 and SV2 utilize a 3-point object correlation function, which considers the information shared between them. This correlation process significantly enhances the confidence level in establishing a correlation with the known database.
- **Step 8: Final Correlation Determination:** If the object is now correlated with the known database based on the collaborative effort of SV1 and SV2, the process concludes successfully. Ground operations may request confirmed correlations be communicated for updates to database observation (i.e., more frequent observations to increase database fidelity).
- **Step 9: Ground Communication for Resolution:** In the event of an unresolved correlation, SV1 and/or SV2 relay the situation to the ground, where operators can assess the information and make informed decisions based on the available data.

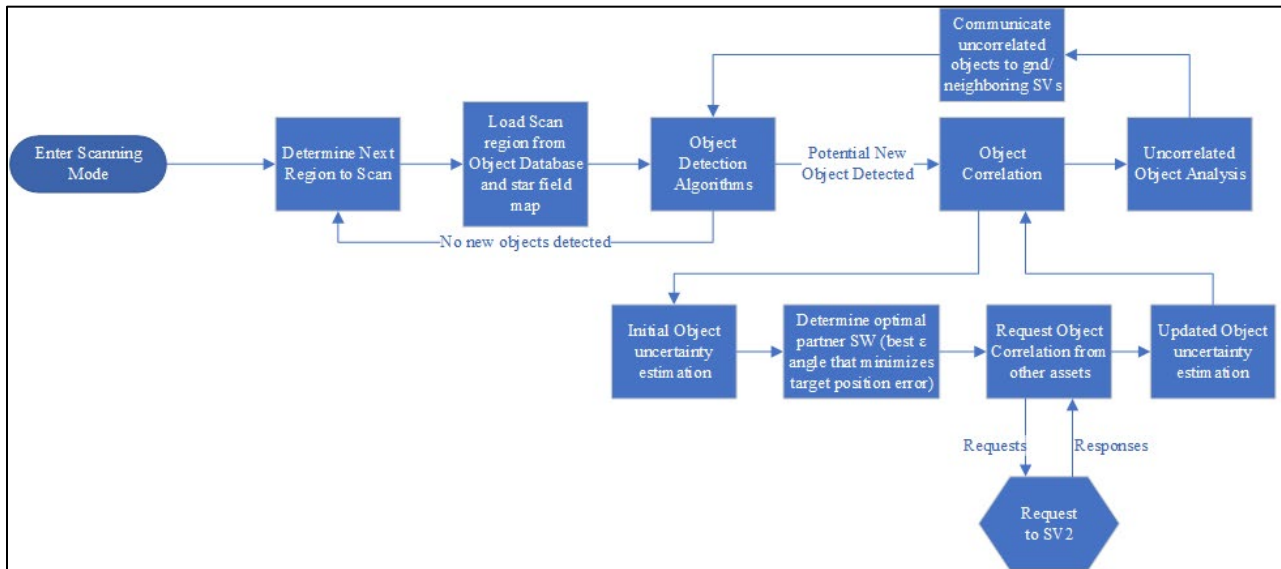


Fig. 15. Sensor Step-Stare Scanning Mode

**Active Tasking Mode:** the active tasking mode follows a process similar to the automatic scanning mode but includes tasks associated with determining if this task can be completed within the time needed and communicating back to the requester status of completing the task any information associated with task completion.

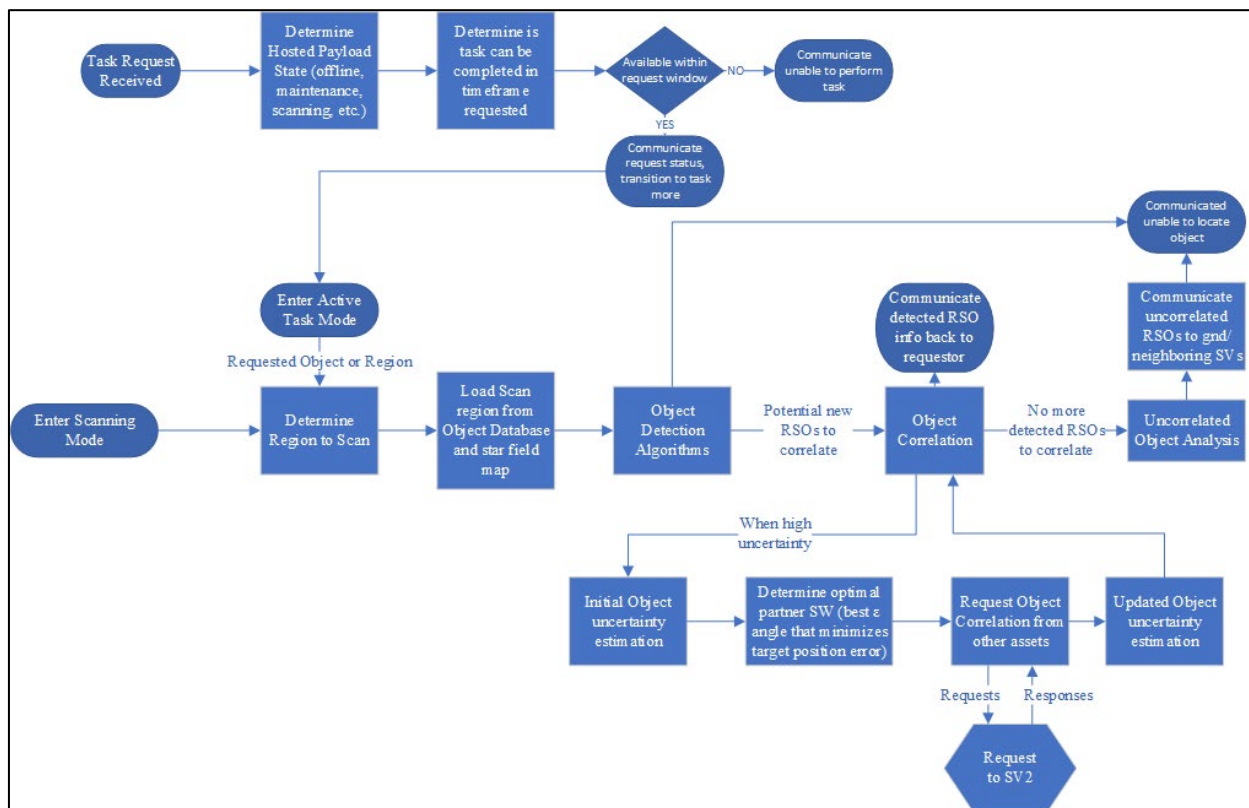
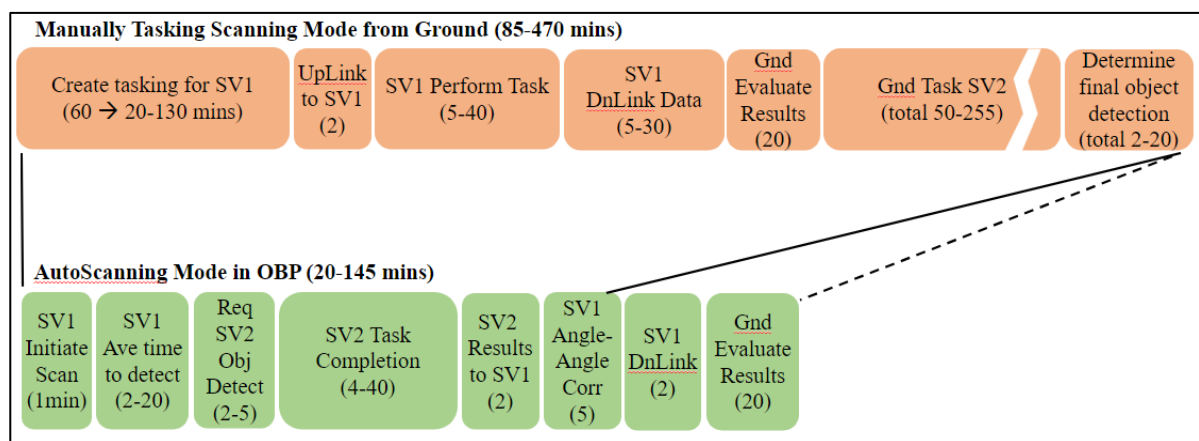


Fig. 16. Sensor Active Tasking Mode

## 7.5 IMPACT OF ON BOARD PROCESSING (OBP) ON THE PROPOSED MISSION SYSTEM ARCHITECTURE

In this section, we have explored the potential use of onboard processing (OBP) within hosted payloads providing space domain awareness in MEO to enable advanced operational concepts (CONOPs) that were previously impractical with ground command and control (C2) systems. The advantages of OBP are substantial and can significantly enhance the effectiveness of SDA architectures.

One of the key benefits of OBP is its ability to facilitate near real-time tip-n-cue coordination, enabling space vehicles (SVs) to rapidly acquire angle-angle track custody of highly maneuverable resident space objects (RSOs). This expedited validation of uncorrelated objects translates into quicker threat detection and notification to operators, circumventing the lengthy delays that conventional systems entail. **Figure 17** depicts this estimated time savings for scanning mode to find and correlating an object to a known database RSO. Note that even if the detected object is not fully coordinated and requires it to be sent to the ground for further processing (dashed line in **Figure 17**), there is still significant time savings. Note that actual savings depends on the amount of data being downloaded, how many ground entry points are accessible at a given time, etc.



**Fig.**

**17. Sensor Auto Scan Mode Timing.** An approximate comparison of Scanning mode for both a classical ground C2 system and the semi-autonomous OBP auto scanning mode. The solid lines correspond to the time to correlate, the dashed line captures extra steps should the ground request download of this activity.

Furthermore, onboard processing reduces operator workload through autonomous and semi-autonomous operations, thereby streamlining the operational process. This efficiency is particularly notable when compared to ground-based operations, which require intricate coordination of ground assets and an increased utilization of up/downlink bandwidth. The OBP approach simplifies the architecture, leading to a more streamlined and effective system.

An additional advantage lies in the potential for the proliferation of SSA/SDA sensors, which are often constrained by operator workload and communication bandwidth limitations. OBP's autonomous operation opens the door to exploring new CONOPs and expanding the capabilities of SDA/SDA systems, further enhancing their utility and impact. Over-the-air update capabilities of both firmware and software in the OBP allows an evolutionary approach. Enhanced, or entirely new paradigms, can be explored and validated using ground based digital twins.

Although there many advantages, we also acknowledge that there are certain challenges associated with OBP adoption. The inclusion of OBP as a hosted payload introduces additional size, weight, power, and cost considerations, which may deter commercial operators from embracing this approach. Additionally, continuous updates to the two-line database of RSOs necessitate uplink bandwidth, potentially limiting the commercial operator's operational capacity.

Despite these challenges, the benefits of OBP in enabling advanced CONOPs, reducing operator workload, and expanding SSA/SDA capabilities make it a promising avenue for future exploration. With the ability to evolve through over-the-air firmware and software updates, OBP allows for a dynamic and adaptive approach, empowering ground-based digital twins to validate new paradigms and enhancements. As technology advances and the space domain evolves, the integration of onboard processing holds the potential to revolutionize the landscape of space situational awareness.

## 8 CONCLUSIONS AND RECOMMENDATIONS

**Market Advantage:** The MEO hosted sensor marketplace has growing value, because launch costs to MEO continue to shrink, global SATCOM constellations such as O3B, Intelsat, and Mangata find low-MEO attractive, Russian, Chinese, and US GPS constellations reside in high-MEO, and affordable space tug capability continues to grow. As a result, the MEO satellite market is projected to be worth USD \$9.52 billion by 2030, growing at a CAGR of 4.7% from 2023 to 2030.

**Diverse Observer Advantage:** MEO provides a clear line of sight to GEO, which is important for monitoring objects in this critical orbit. MEO has a lower background of objects than LEO, which makes it easier to track and identify objects. MEO has a longer dwell time on objects, which allows for more accurate tracking.

**High vs. Low MEO Pros and Cons:** The use of GPS (high-MEO) and Mangata, O3B, and Intelsat (low MEO) satellites to host SDA sensors is explored. GPS satellites have a longer revisit rate but lower quality observations, while low-MEO satellites have a shorter revisit rate but higher quality observations. The optimal altitude for an SDA constellation depends on the mission. For GEO SSA, the optimal altitude is approximately 29,270 km, while for LEO SSA, the optimal altitude is approximately 312 km. A mix of high and low MEO-hosted SDA sensors is wise.

**States and Modes Conclusions:** The LEO, MEO, GEO, xGEO belt background scan modes are autonomous and enable full sensor utilization 24 x 7 when not servicing time-sensitive active tasks. The scanning modes are able to detect objects that are not in the known database, such as. Near Earth Orbit (NEO) asteroid detection missions. The scanning modes can use tip/que coordination with other sensors in the SDA architecture to improve the accuracy of object position determination and correlation at global MOCs.

**Hosted Onboard processing (OBP) and Sensing:** can greatly reduce the data communication bandwidth cost required for hosted SDA missions. OBP allows the satellite to only downlink important information, such as information about new or unknown objects. OBP can provide more timely and accurate information to operators. This can be critical for missions that require rapid response to threats, such as collision avoidance with debris or threats. Our proposed OBP hardware architecture consists of a flexible mix of instruction set processing, storage, and FPGA slices. The instruction set processing slices use commercial microprocessors that have been demonstrated to be radiation tolerant in the MEO environment. The storage slices use non-volatile memory (NVM) with 2-3 Terabytes of capacity. The FPGA slices use SRAM based reprogrammable FPGAs and SONOS Flash based FPGAs that retain their configuration over a power cycle. OBP with on board sensing has some drawbacks such as increased SWaPC of the host vehicle and increased integration complexity of the host vehicle. Overall, OBP and hosted sensing is a promising technology for SDA missions. Overall, OBP and hosted sensing in MEO is likely to provide resilience and SDA data sales revenue in the coming decades as launch capacity grows and as LEO and GEO become congested.

## 9 REFERENCES

[1] Di Wu, Aaron J. Rosengren. (2021) *RSO Proper Elements for Space Situational and Domain Awareness*. University of California San Diego, La Jolla, CA, United States.

[2] McKinsey contributors. (January 2022). [www.mckinsey.com](http://www.mckinsey.com), *Space: Investment shifts from GEO to LEO and now beyond*. Retrieved from [Space: Investment shifts from GEO to LEO and now beyond | McKinsey](https://www.mckinsey.com/industries/aerospace-and-defense/our-insights/space-investment-shifts-from-geo-to-leo-and-now-beyond)

[3] Data Bridge Market Research. "Global Medium Earth Orbit (MEO) Satellite Payload Market – Industry Trends and Forecast to 2028". <https://www.databridgemarketresearch.com/reports/global-medium-earth-orbit-meo-satellite-payload-market>

[4] Blake, Travis, Sánchez, Michael, Bolden, and Mark. *OrbitOutlook: Data-centric Competition Based Space Domain Awareness (SDA)*. [https://www.spacesymposium.org/wp-content/uploads/2017/10/T.Blake\\_30th\\_Space\\_Symposium\\_Tech\\_Track.pdf](https://www.spacesymposium.org/wp-content/uploads/2017/10/T.Blake_30th_Space_Symposium_Tech_Track.pdf), 2027

[5] Williamson-Smith, UPWARD Magazine of the ISS National Lab, <https://www.issnationallab.org/hpe-supercomputing-return-space/>



[6] Krantz, H., Pierce, E.C. & Block, A. (2022) *Characterization of LEO satellites with all-sky photometric signatures*. Steward Observatory, University of Arizona.

[7] Liu, D., Chen, B., Chin, T.-J., & Rutten, M. (2020). *Topological sweep for multi-target detection of geostationary space objects*. IEEE Transactions on Signal Processing, 68.

[8] Koblick, D. C., & Choi, J. S. (2023, March). *Cislunar orbit determination benefits of moon-based sensors*. Paper presented at the 2022 Maui AMOS Conference. Paper retrieved at [Koblick\\_2.pdf \(amostech.com\)](#)